Facial Plastic Surgery
&Aesthetic Medicine

ORIGINAL INVESTIGATION | **Rhinoplasty**

Gender Differences in Nasal Anatomy and Function Among Caucasians

Sarah M. Russel, MD[1] and Dennis O. Frank-Ito, PhD[2–4,*]

Abstract

Background: Anatomical variations influence nasal physiology, yet sex differences in physiology remains unclear.

Objective: To investigate sex differences among Caucasians using computational fluid dynamics.

Methods: Adult subjects were selected with normal nasal cone beam computed tomography (CBCT) images and Nasal Obstruction Symptom Evaluation scores ≤30. The CBCT images were used to create subject-specific airway models. Nasal surface area (SA) and volume were computed, and airflow and heat transfer were simulated.

Results: The CBCT scans were taken from 23 females and 12 males. The SA and volume (males: mean = 25.0 cm^3; females: mean = 19.5 cm^3; $p < 0.001$; Cohen's $d = 1.51$) were significantly larger for males, but SA-to-volume ratio did not differ significantly. Although unilateral nasal resistance did not vary greatly, females had higher bilateral resistance (males: mean = 0.04 Pa.s/mL; females: mean = 0.05 Pa.s/mL; $p = 0.044$; Cohen's $d = 0.37$). Females had higher heat flux (males: mean = 158.5 W/m^2; females: mean = 191.8 W/m^2; $p = 0.012$; Cohen's $d = 0.79$), but males had larger SA where mucosal heat flux exceeds 50 W/m^2.

Conclusions: These findings suggest differences in normal nasal anatomy and physiology between Caucasian males and females, which may be useful when assessing sex-specific functional outcomes after nasal surgery.

Introduction

Variability in human nasal anatomy, including nasal cycle, nasal vestibule morphological phenotypes, and nasal index (NI), influences normal nasal airflow.[1–6] The nasal cycle is a temporal variation induced by spontaneous, reciprocal fluctuation of nasal patency associated with phases of congestion and decongestion of nasal mucosa.[5] The typical duration of a nasal cycle is between 30 min and 6 h.[7] Another source of variability involves nasal vestibule morphological shapes—Notched, Standard, and Elongated.[3]

The Notched phenotype has a prominent notch at the junction of the ala and sidewall; the Standard phenotype is considered the ''typical'' formation; and the Elongated phenotype is slightly elongated at the level of the nasal ala.[3] Lastly, NI, which is attributed to variations in climatic conditions, is the ratio of nasal width to nasal height. An NI of <70 is known as leptorrhine, >85 is platyrrhine, and 70–85 is mesorrhine, with Caucasian populations often having leptorrhine anatomy and African populations having platyrrhine.[2]

[1]Department of Otolaryngology/Head & Neck Surgery, University of North Carolina—Chapel Hill, Chapel Hill, North Carolina, USA.
[2]Department of Head and Neck Surgery & Communication Sciences, Duke University Medical Center, Durham, North Carolina, USA.
[3]Department of Mechanical Engineering and Materials Science, Duke University, Durham, North Carolina, USA.
[4]Computational Biology and Bioinformatics PhD Program, Duke University, Durham, North Carolina, USA.

*Address correspondence to: Dennis O. Frank-Ito, PhD, Department of Head and Neck Surgery & Communication Sciences, Duke University Medical Center, 40 Duke Medicine Circle, DUMC Box 3805, Durham, NC 27710, USA, Email: dennis.frank@duke.edu

KEY POINTS

Question: Are there sex differences in normal nasal anatomy and physiology within a Caucasian population?

Findings: Males have significantly larger nasal passages and significantly lower total nasal resistance (NR) to airflow.

Meaning: Our findings suggest baseline differences in nasal anatomy and physiology between Caucasian males and females, which surgeons may use when assessing gender-specific outcomes after nasal surgery.

Although anatomic variations among ethnicities have been widely studied, less is known about sex differences in nasal airway anatomy within ethnicities. Although certain anatomical differences are known, they are largely differences in bony dimensions and facial angles within the realm of facial plastics.[8] After standardizing for size, males are considered to have larger airway passages than females.[9] Namely, males showed relatively taller piriform apertures, nasal cavities, and choanae than females, which contributed to this difference.[9] In addition, men may have lower nasal airway resistance than females.[10]

With regard to race and nasal patency, individuals from African descents are reported to have lower nasal resistance (NR) than Caucasians, but studies debate whether this difference is statistically significant.[11,12] Another study noted differences in nasal airflow patterns between a Caucasian male subject and an Indian male subject.[4]

Nonetheless, little is known about nasal anatomical differences between sexes and how these differences correlate to nasal function. If race and sex are confounding factors in physiological differences across studies, differences in anatomical variations and nasal function between sexes could be concisely investigated within one racial group. The objective of this study is to investigate sex differences in nasal anatomy and function within the Caucasian population using computational fluid dynamics (CFD) modeling. CFD modeling is a powerful tool for examining these discrepancies, as it allows for a comprehensive investigation into how anatomical differences affect nasal airflow profiles.[13–15] Lastly, CFD provides information about localized behavior not captured in other settings, such as determining which aspects of airway anatomy cause sex differences in overall airway physiology.

Methods
Study subjects
This retrospective study, approved by the Duke University Health System Institutional Review Board, involves 35 healthy Caucasian adult subjects with high resolution cone beam computed tomography (CBCT) images of the head and neck. Inclusion criteria: (1) a score of ≤30 on the validated patient-reported Nasal Obstruction Symptom Evaluation (NOSE) questionnaires; (2) ≥18 years old and Caucasian; (3) non-smokers; (4) available CBCT of the head and neck region; and (5) radiographic evidence of normal nasal passage.[1,16] Radiographic exclusion criteria included septal deviation >5°, septal perforation, evidence of sinusitis, and significant nasal cycling at the time of the scan causing a unilaterally decreased airspace.[17] Other exclusion criteria included previous sinus surgery or comorbid pathology affecting the nasal cavity or paranasal sinuses.

Nasal airway reconstruction
Radiographic images of each subject's nasal passage obtained from CBCT scans were read into imaging analysis software MIMICS™ 17.0 (Materialise Inc., Leuven, Belgium) for creation of anatomically realistic and subject-specific three-dimensional models of nasal airways. Our models excluded paranasal sinuses, as airflow through natural ostia to the sinuses can be considered negligible relative to the nasal cavity and would not influence nasal airflow dynamics other than increasing the volume of these models. Airway models were segmented using Hounsfield unit threshold −1024HU to −300HU, with subsequent manual editing as needed, similar to our previously published models.[1,18–20]

Nasal airflow simulations
After subject-specific nasal models were created, hybrid tetrahedral-prismatic mesh elements were generated in nasal cavities for each subject using ICEM-CFD 19.0 (ANSYS, Inc., Canonsburg, PA), which is necessary for the simulation of nasal airflow and heat transfer. Approximately 4 million unstructured tetrahedral elements and fine three-layer prism elements were generated in each nasal cavity. Mesh refinement analysis was deemed unnecessary for this study, as our choice of mesh density is consistent with our prior publication on mesh refinement analysis, which demonstrated that mesh independent numerical results showed asymptotic behavior starting at 4 million elements.[21] Mesh quality analysis was performed to ensure that elements with poor aspect ratio in the hybrid mesh were smoothed to prevent distorted elements from impacting the accuracy of the numerical simulation.

Steady-state, laminar inspiratory airflow was simulated in nasal cavities using the CFD software package, Fluent 19.0 (ANSYS, Inc.) to mimic physiological inhalation conditions at 15 L/min.[1,22,23] Given that flow velocities through the nasal cavity during low-to-moderate breathing typically have a Mach number <<0.2, the governing equations of fluid flow reduces to:

$$\nabla \cdot \vec{u} = 0,$$

$$\rho(\vec{u} \cdot \nabla)\vec{u} = -\nabla p + \mu \nabla^2 \vec{u},$$

where $\vec{u} = \vec{u}(x, y, z)$ is velocity vector field, $\rho = 1.204$ kg/m^3 is fluid density, $u = 1.825 \times 10^{-5}$ kg/m $-$ s is dynamic viscosity, and ρ is pressure. The thermal energy and species transport equations for heat transfer and water vapor are defined as

$$(\vec{u} \cdot \nabla)T = \frac{k}{\rho c_p} \nabla^2 T,$$

where $T = T(x, y, z)$ is temperature, $k = 0.0268$ W/m-K is thermal conductivity, and $c_p = 1005.9$ J/kg-K is specific heat of air. Airflow and heat transfer simulations were performed using these boundary conditions: (1) at the nasal wall, no-slip, stationary wall, temperature was set at 32.6°C; (2) at the inlet, a ''pressure-inlet'' with gauge pressure set to zero, temperature at 20°C; and (3) a ''mass-flow-outlet'' condition at the outlet to target 0.000301 kg/s (15 L/min), with temperature set to 32.6°C.

Computed quantities of interest

To determine the patency of each nasal cavity, NR was calculated as $\Delta P/Q$ (Pa.s/mL) where ΔP is bilateral/unilateral pressure drop from nostrils to choana, and Q is bilateral/unilateral volumetric flow rate. In addition, the volume and surface area (SA) of the nasal airway were calculated, as well as nasal mucosa heat flux, which is the rate of heat loss across the nasal mucosa during inspiration; and the SA stimulated by mucosal cooling, which is defined by the mucosa SA where heat flux exceeds 50 W/m^2 (SAHF50).[1,24]

Summary statistics comprising means, standard deviations (SDs), and median were reported for all variables of interest. To measure the strength of the relationship between males and females across computed variables, the effect size was calculated using Cohen's d. Statistical analysis was performed using the Non-Parametric Wilcoxon Rank Sum test, and all comparisons were examined for statistical significance at $\alpha = 0.05$.

Necessary power calculations were performed at $\alpha = 0.05$ using the two sample Satterthwaite unpooled t-test on the mean difference between males and females, assuming unequal variances. Power analysis was calculated for the following variables: nasal volume difference; nasal SA difference; nasal SA-to-volume (SA:V) ratio difference; nasal unilateral airflow difference; nasal unilateral resistance difference; nasal bilateral resistance difference; nasal heat flux combined difference; and nasal SAHF50 combined difference.

Results

Demographics

There were 35 subjects in this study—12 males and 23 females. Representative female and male nasal airways are depicted in Figure 1A and B, respectively. As indicated in Figure 1C, groups were similar in age—median ages were 61 years for males (mean = 52.4 years, SD = 18.8 years) and 52 years for female (mean = 49.2 years, SD = 16.7 years); the age difference between sexes was not statistically significant ($p = 0.639$; Cohen's $d = 0.18$). However, they differ significantly ($p < 0.001$; Cohen's $d = 1.69$) in weight; males weighed more than females (males: median = 90 kg, mean = 94 kg, SD = 14.4 kg; females: median = 68 kg, mean = 68.7 kg, SD = 15.3 kg; Fig. 1D).
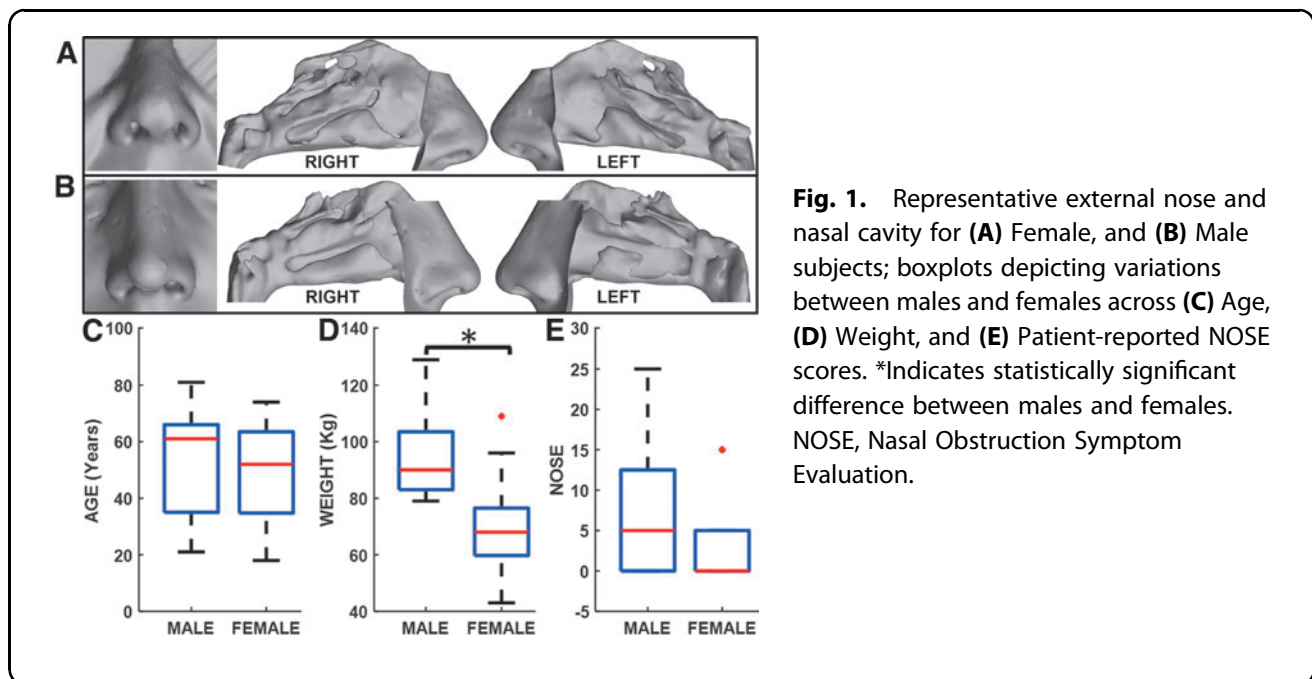
Fig. 1. Representative external nose and nasal cavity for **(A)** Female, and **(B)** Male subjects; boxplots depicting variations between males and females across **(C)** Age, **(D)** Weight, and **(E)** Patient-reported NOSE scores. *Indicates statistically significant difference between males and females. NOSE, Nasal Obstruction Symptom Evaluation.

In addition, NOSE scores were not significantly different ($p = 0.166$; Cohen's $d = 0.62$; Fig. 1E); median NOSE scores were 5 for males (mean $= 7.5$, SD $= 8.0$) and 0 (mean $= 3.7$, SD $= 4.9$) among females.

Nasal anatomy

In Figure 2A, males had a significantly ($p < 0.001$; Cohen's $d = 1.51$; power $= 98.5\%$) greater nasal airway volume (males: median $= 24.2$ cm^3, mean $= 25.0$ cm^3, SD $= 3.5$ cm^3; females: median $= 18.4$ cm^3, mean $= 19.5$ cm^3, SD $= 3.7$ cm^3). Similarly, males had a significantly ($p < 0.001$; Cohen's $d = 1.80$; power $= 99.6\%$; Fig. 2B) larger nasal SA than females (males: median $= 204.1$ cm^2, mean $= 211.6$ cm^2, SD $= 20.2$ cm^2; females: median $= 183.0$ cm^2, mean $= 178.1$ cm^2, SD $= 17.7$ cm^2). Comparison of nasal SA:V ratio between sexes was not statistically different (median: males $= 8.6$ cm^{-1}, females $= 9.4$ cm^{-1}; $p = 0.106$; Cohen's $d = 0.61$; power $= 48.8\%$); females had higher SA:V than males. Females also had greater variability in SA:V (Fig. 2C).

Nasal airflow profile

Unilateral nasal airflow results presented in Figure 2D–F indicated that male and female subjects had similar flow rates on both the left (Fig. 2D) and right (Fig. 2E). Median flow rate was 7.5 L/min in each nasal airway for males, whereas females had median flow rates of 7.4 L/min and 7.6 L/min on the left and right sides, respectively. As demonstrated in Figure 2F, comparison of unilateral airflow differences between sides for males and females showed greater unilateral airflow difference in males than females (males: median $= 4.7$ L/min, mean $= 4.4$ L/min, SD $= 2.7$ L/min; females: median $= 2.3$ L/min, mean $= 2.7$ L/min, SD $= 2.4$ L/min), but this difference was not statistically significant ($p = 0.068$; Cohen's $d = 0.68$).
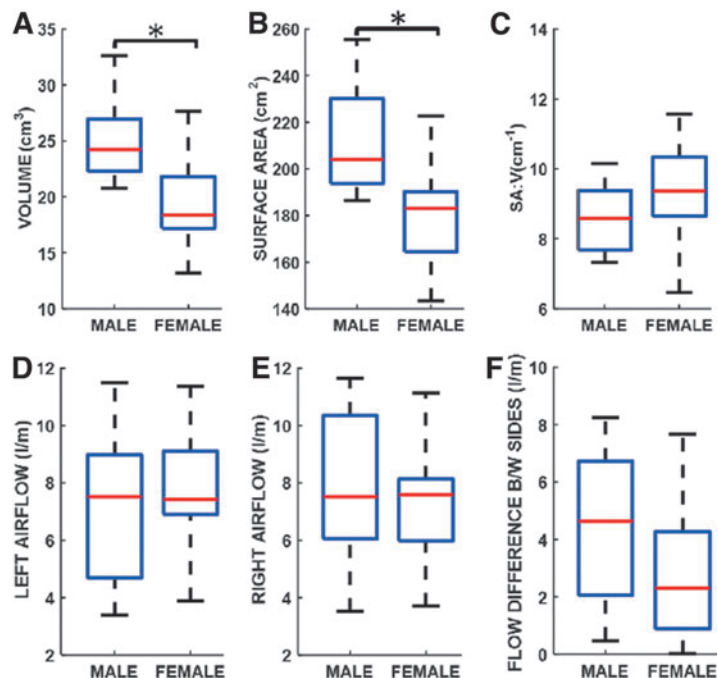
Figure 3A and B showed that unilateral NR distribution was higher on both sides of the airways in females (left: median $= 0.09$ Pa.s/mL; right: median $= 0.10$ Pa.s/mL) than males (left: median $= 0.07$ Pa.s/mL; right: median $= 0.06$ Pa.s/mL). Contrarily, unilateral resistance difference between both nasal airways indicated a marginal nonsignificant increase among males than females ($p = 0.476$; Cohen's $d = 0.42$; power $= 41.6\%$; males: median $= 0.04$ Pa.s/mL, mean $= 0.06$ Pa.s/mL, SD $= 0.06$ Pa.s/mL; females: median $= 0.04$ Pa.s/mL, mean $= 0.04$ Pa.s/mL, SD $= 0.04$ Pa.s/mL; Fig. 3C).
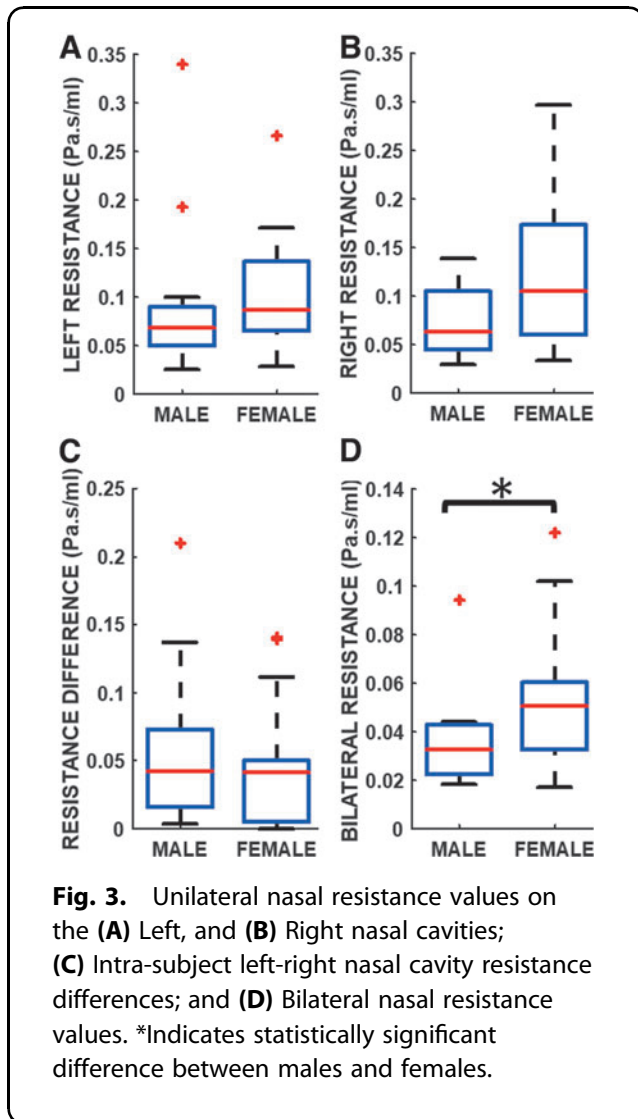
Bilateral NR between sexes was significant difference ($p = 0.044$; Cohen's $d = 0.37$; power $= 20.5\%$); females had greater resistance than males (males: median $= 0.03$ Pa.s/mL, mean $= 0.04$ Pa.s/mL, SD $= 0.02$ Pa.s/mL; females: median $= 0.05$ Pa.s/mL, mean $= 0.05$ Pa.s/mL, SD $= 0.03$ Pa.s/mL; Fig. 3D). Further, nasal airflow streamlines are displayed in Figure 4A for representative female and male subjects.

Nasal heat transfer

Figure 4B and C show heat flux color maps on the nasal lateral wall (Fig. 4B) and septal wall (Fig. 4C) for representative female and male subjects. Distribution of average heat flux across unilateral left and right nasal mucosa

Fig. 2. Nasal anatomy comparisons between males and females for **(A)** Nasal volume, **(B)** Nasal surface area, and **(C)** Nasal surface-area-to-volume ratio. Unilateral airflow volume on the **(D)** Left, and **(E)** Right nasal cavities; and **(F)** Intra-subject left-right nasal cavity airflow differences. *Indicates statistically significant difference between males and females.

Fig. 3. Unilateral nasal resistance values on the **(A)** Left, and **(B)** Right nasal cavities; **(C)** Intra-subject left-right nasal cavity resistance differences; and **(D)** Bilateral nasal resistance values. *Indicates statistically significant difference between males and females.

higher ($p = 0.012$; Cohen's $d = 0.79$; power = 54.5%) mucosa heat flux distribution than males (males: median = 148.7 W/m^2, mean = 158.5 W/m^2, SD = 44.1 W/m^2; females: median = 194.1 W/m^2, mean = 191.8 W/m^2, SD = 40.7 W/m^2; Fig. 5C).
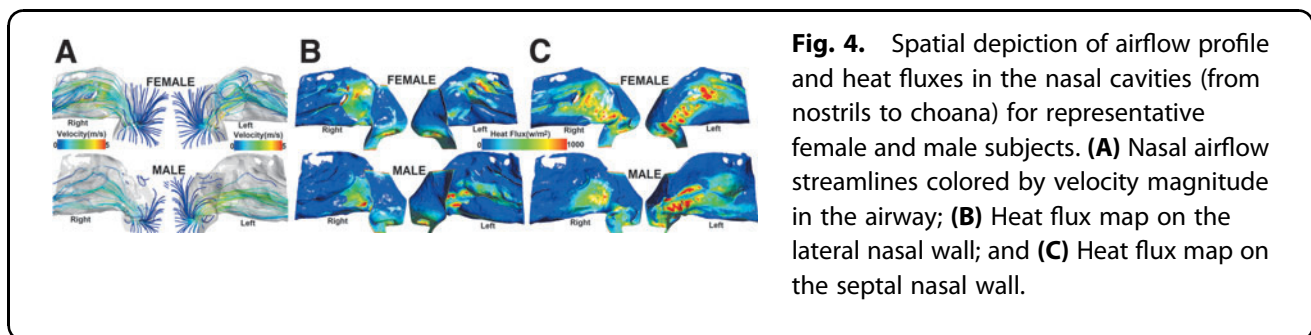
SAHF50 boxplots are presented in Figure 5D–F. Males median SAHF50 values were 50.9 cm^2 (left) and 53.5 cm^2 (right), compared with 46.2 cm^2 (left) and 41.3 cm^2 (right) among females (Fig. 5D, E). SAHF50 after combining left and right datasets was significantly different yet underpowered ($p = 0.031$; Cohen's $d = 0.54$; power = 25.5%) between males and females, with males having larger SAHF50 (males: median = 51.7 cm^2, mean = 50.4 cm^2, SD = 11.4 cm^2; females: median = 45.8 cm^2, mean = 45.3 cm^2, SD = 8.2 cm^2; Fig. 5F).

Discussion

These results highlight important similarities and differences in nasal anatomy and function between males and females within the Caucasian population. Variations among ethnicities have been previously studied, but this work fills an important gap in describing the differences between sexes in a homogenous racial group. These findings demonstrate that Caucasian males have significantly larger nasal volumes and SA than Caucasian females. In addition, unilateral NR was similar between sexes, but bilateral NR was significantly higher for females than males.

Females also showed significantly greater average heat flux than males with a large effect size, but males had a greater SAHF50 with a moderate effect size. The values reported may be used when assessing sex-specific anatomical and functional outcomes from nasal surgery within a Caucasian patient population.

Our findings suggest that male patients have larger SA and nasal volume compared with females. Our results are congruent with previous work suggesting that males have larger noses due to taller piriform apertures, internal nasal cavities, and choanae.[9] Of note, Cohen's d measures effect size for each variable studied, with 0.01 designating very small effect, 0.2 small effect, 0.5 medium effect, 0.8 large effect, and anything >1.2 very large effect.[25] The d-values for SA and volume were 1.80 and 1.51,

showed less variability and higher median heat flux among females (left: median = 194.8 W/m^2; right: median = 189.9 W/m^2) than males (left: median = 158.2 W/m^2; right: median = 148.7 W/m^2; Fig. 5A, B).

Comparison of unilateral heat flux after combining left and right datasets showed that females had a significantly

Fig. 4. Spatial depiction of airflow profile and heat fluxes in the nasal cavities (from nostrils to choana) for representative female and male subjects. **(A)** Nasal airflow streamlines colored by velocity magnitude in the airway; **(B)** Heat flux map on the lateral nasal wall; and **(C)** Heat flux map on the septal nasal wall.

Fig. 5. Nasal cavity average mucosal heat flux values on the **(A)** Left, **(B)** Right, and **(C)** combing data for the unilateral left and right nasal cavities; SAHF50 on the **(D)** Left, **(E)** Right, and **(F)** combing data for the unilateral left and right nasal cavities. *Indicates statistically significant difference between males and females. SAHF50, surface area where mucosal heat flux exceeds 50 W/m^2.
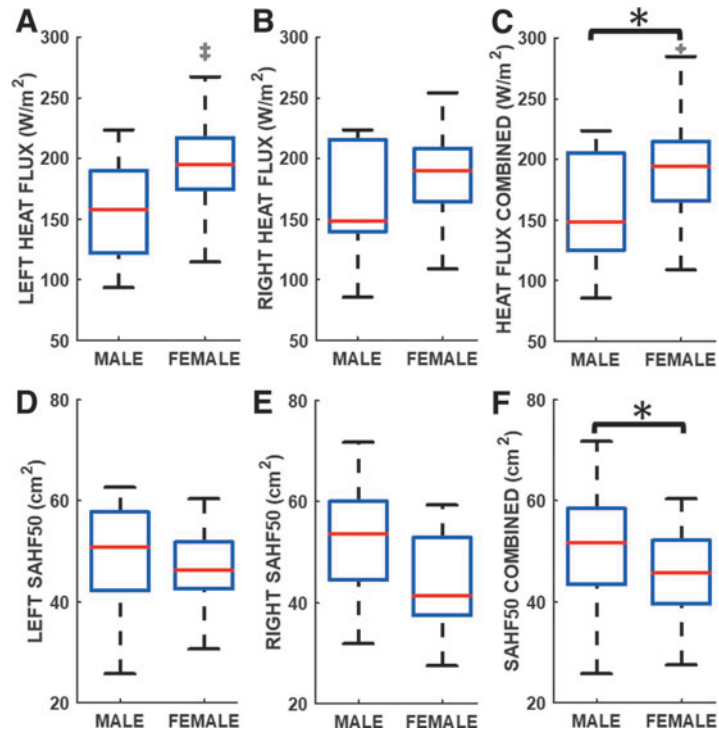
respectively, which indicates a very strong and realistic difference in nasal SA and volume between sexes.

Nonetheless, the SA:V ratio between sexes was not significantly different with an effect size of 0.61, suggesting that Caucasian males and females have comparable capacity for heating and humidifying their nasal mucosa relative to their respective nasal volumes.[26] Larger SA:V is associated with greater nasal SA exposure to heat and moisture transfer for a given nasal volume.[26]

In addition, these results demonstrated no significant difference in unilateral nasal airflow between sexes, but female subjects did have higher bilateral NR than males. Notably, for both males and females, nasal airflow on each side was almost exactly half the airflow during quiet breathing (7.5 L/min from total of 15 L/min), which is expected in subjects with a healthy nasal passage and no evidence of nasal airway obstruction.[27] In previous models of nasal airflow in healthy individuals, normal unilateral airflow ranged from 3.6 to 11.5 L/min ±1.2 L/min, and our values fall in the middle of this range.[1]

With bilateral NR between sexes, average difference yielded a small-to-medium effect size. Our findings parallel those from previous computational models and rhinomanometry measurements in healthy individuals.[1,28] Further, in previous work measuring nasal airflow resistance with rhinomanometry, NR was lower in males than females, correlating with our findings.[10] The impact of bilateral NR on patients' perception of nasal patency is unclear. Previous works comparing bilateral NR to symptoms of nasal obstruction reported little correlation between the two.[22,29] Unilateral NR and airflow, however, have stronger correlation with obstructive symptoms when compared with bilateral NR.[22,30]

Thus, further work remains to elucidate the impacts of increased bilateral NR on pathologies in females compared with males. These variables may correlate with patients' reported perception of nasal patency, with larger SA where heat flux values are >50 W/m^2 and greater heat flux values corresponding with increased perception of airflow.[22,30,31]

Similar to our prior publication,[1] the present study provides information about baseline values and relative differences in nasal anatomy and physiology between Caucasian male and female subjects, allowing for more precise future comparisons between sexes and gender-specific normative ranges of nasal function to target during surgical correction of nasal obstruction. Norms for assessing outcomes from nasal surgery are not well established, particularly well-evaluated clinical variables that correlate with patients' perceptions of normal nasal function.

Current evaluation of outcomes after nasal surgery relies on facial analysis, which uses predetermined angles and assessment of symmetry to determine aesthetic outcomes. However, these techniques do not examine functional outcomes for patients, which could ultimately impact patients' quality of life after nasal surgery. This

work provides greater insight into normal nasal physiology in each sex, which allows for a foundation on which to build tools to assess functional outcomes after nasal surgery.

This work has its limitations, such as examining only one ethnic group. Although the sample size is large for a CFD study, male and female subjects are not equally represented. To develop a strong normative baseline that provides gender-specific targets for surgeons, an increased sample size would generate stronger statistical power. Our simulations were conducted with a single flow rate, 15 L/min, at steady state, which is useful to understand airflow dynamics during quiet inspiration.

Conducting transient simulations would have provided insight into respiratory cycles, but we did not perform these during this study due to the volume of data produced and the time required to run these simulations. For instance, steady-state simulations take 10–12 h to run per subject, but transient simulations take at least 100 h per subject to run at a time step of 10^{-4} for 2 s. Consequently, we decided to use steady state for this study but recognized the merit of conducting transient simulations for more detailed data in future work.

Conclusion
The CFD modeling was used to investigate baseline variations in nasal anatomy and physiology between sexes in a Caucasian population. By conducting this work within one ethnicity, anatomical and physiological variations among ethnic groups are controlled. Nasal airflow was similar between sexes, but female subjects had greater bilateral NR than males. Although results suggest that male subjects have greater nasal SA and volume, SA:V ratio was not significantly different. Females had greater average mucosal heat flux, but males had larger SAHF50.

Our findings can be used as a foundation for assessing sex-specific outcomes of nasal surgery within Caucasians. Future work includes investigating sex variations in nasal anatomy and physiology within other ethnic groups to determine whether the results presented here for Caucasians differ significantly from other groups.

Acknowledgments
Special thanks are due to ANSYS, ANSYS Global Academic Program, and Dr. Paolo Maccarini (Duke University) for support and strategic donation. All authors gave final approval for publication.

Disclaimer
The content is solely the responsibility of the authors and does not necessarily represent the official views of the National Institutes of Health.

Author Disclosure Statement
The authors have no conflicts of interest to disclose.

References
1. Borojeni AAT, Garcia GJM, Moghaddam MG, et al. Normative ranges of nasal airflow variables in healthy adults. *Int J Comput Assist Radiol Surg.* 2020;15:87–98.
2. Leong S, Eccles R. A systematic review of the nasal index and the significance of the shape and size of the nose in rhinology. *Clin Otolaryngol.* 2009;34:191–198.
3. Ramprasad VH, Frank-Ito DO. A computational analysis of nasal vestibule morphologic variabilities on nasal function. *J Biomech.* 2016;49:450–457.
4. Zhu JH, Lee HP, Lim KM, Lee SJ, Wang DY. Evaluation and comparison of nasal airway flow patterns among three subjects from Caucasian, Chinese and Indian ethnic groups using computational fluid dynamics simulation. *Respir Physiol Neurobiol.* 2011;175:62–69.
5. Eccles R. A role for the nasal cycle in respiratory defence. *Eur Respir J.* 1996;9:371–376.
6. Frank-Ito DO, Garcia G. Clinical implications of nasal airflow simulations. In: Inthavong K, Singh N, Wong E, Tu J, eds. *Clinical and Biomedical Engineering in the Human Nose.* Singapore: Springer; 2021:157–192.
7. Gungor A, Moinuddin R, Nelson RH, Corey JP. Detection of the nasal cycle with acoustic rhinometry: techniques and applications. *Otolaryngol Head Neck Surg.* 1999;120:238–247.
8. Hwang TS, Song J, Yoon H, Cho BP, Kang HS. Morphometry of the nasal bones and piriform apertures in Koreans. *Ann Anat.* 2005;187:411–414.
9. Bastir M, Godoy P, Rosas A. Common features of sexual dimorphism in the cranial airways of different human populations. *Am J Phys Anthropol.* 2011;146:414–422.
10. Ren L, Zhang L, Duan S, Zhang W, Zhang Y. Nasal airflow resistance measured by rhinomanometry in a healthy population of China. *Int Forum Allergy Rhinol.* 2018;8:1308–1314.
11. Ohki M, Naito K, Cole P. Dimensions and resistances of the human nose—racial-differences. *Laryngoscope.* 1991;101:276–278.
12. Canbay EI, Bhatia SN. A comparison of nasal resistance in white Caucasians and blacks. *Am J Rhinol.* 1997;11:73–75.
13. Inthavong K, Chetty A, Shang Y, Tu J. Examining mesh independence for flow dynamics in the human nasal cavity. *Comput Biol Med.* 2018;102:40–50.
14. Basu S, Witten N, Kimbell J. Influence of localized mesh refinement on numerical simulations of post-surgical sinonasal airflow. *J Aerosol Med Pulm Drug Deliv.* 2017;30:14.
15. Pourmehran O, Gorji TB, Gorji-Bandpy M. Magnetic drug targeting through a realistic model of human tracheobronchial airways using computational fluid and particle dynamics. *Biomech Model Mechanobiol.* 2016;15:1355–1374.
16. Rhee JS, Sullivan CD, Frank DO, Kimbell JS, Garcia GJ. A systematic review of patient-reported nasal obstruction scores: defining normative and symptomatic ranges in surgical patients. *JAMA Facial Plast Surg.* 2014;16:219–225; quiz 232.
17. Keeler JA, Patki A, Woodard CR, Frank-Ito DO. A computational study of nasal spray deposition pattern in four ethnic groups. *J Aerosol Med Pulm Drug Deliv.* 2016;29:153–166.
18. Frank-Ito DO, Kimbell JS, Borojeni AA, Garcia GJ, Rhee JS. A hierarchical stepwise approach to evaluate nasal patency after virtual surgery for nasal airway obstruction. *Clin Biomech.* 2019;61:172–180.
19. Patki A, Frank-Ito DO. Characterizing human nasal airflow physiologic variables by nasal index. *Respir Physiol Neurobiol.* 2016;232:66–74.
20. Brandon BM, Austin GK, Fleischman G, et al. Comparison of airflow between spreader grafts and butterfly grafts using computational flow dynamics in a cadaveric model. *JAMA Facial Plast Surg.* 2018;20:215–221.

21. Frank-Ito DO, Wofford M, Schroeter JD, Kimbell JS. Influence of mesh density on airflow and particle deposition in sinonasal airway modeling. *J Aerosol Med Pulm Drug Deliv.* 2016;29:46–56.

22. Kimbell JS, Frank DO, Laud P, Garcia GJ, Rhee JS. Changes in nasal airflow and heat transfer correlate with symptom improvement after surgery for nasal obstruction. *J Biomech.* 2013;46:2634–2643.

23. Garcia GJ, Schroeter JD, Segal RA, Stanek J, Foureman GL, Kimbell JS. Dosimetry of nasal uptake of water-soluble and reactive gases: a first study of interhuman variability. *Inhalat Toxicol.* 2009;21: 607–618.

24. Sullivan CD, Garcia GJ, Frank-Ito DO, Kimbell JS, Rhee JS. Perception of better nasal patency correlates with increased mucosal cooling after surgery for nasal obstruction. *Otolaryngol Head Neck Surg.* 2014;150:139–147.

25. Sawilowsky SS. New effect size rules of thumb. *J Modern Appl Stat Methods.* 2009;8:26.

26. Inthavong K, Ma J, Shang Y, et al. Geometry and airflow dynamics analysis in the nasal cavity during inhalation. *Clin Biomech.* 2019;66:97–106.

27. Subramaniam RP, Richardson RB, Morgan KT, Kimbell JS, Guilmette RA. Computational fluid dynamics simulations of inspiratory airflow in the human nose and nasopharynx. *Inhalat Toxicol.* 1998;10:91–120.

28. Zhao K, Jiang J. What is normal nasal airflow? A computational study of 22 healthy adults. *Int Forum Allergy Rhinol.* 2014;4:435–446.

29. Zhao K, Jiang J, Blacker K, et al. Regional peak mucosal cooling predicts the perception of nasal patency. *Laryngoscope.* 2014;124:589–595.

30. Casey KP, Borojeni AA, Koenig LJ, Rhee JS, Garcia GJ. Correlation between subjective nasal patency and intranasal airflow distribution. *Otolaryngol Head Neck Surg.* 2017;156:741–750.

31. Gaberino C, Rhee JS, Garcia GJM. Estimates of nasal airflow at the nasal cycle mid-point improve the correlation between objective and subjective measures of nasal patency. *Resp Physiol Neurobiol.* 2017;238:23–32.